International Journal of Solids and Structures xxx (xxxx) xxx

Contents lists available at ScienceDirect

International Journal of Solids and Structures

journal homepage: www.elsevier.com/locate/ijsolstr

# Linking micro grainsize polydispersity to macro porosity

Giulia Guida[a,*], Itai Einav[b], Benjy Marks[b], Francesca Casini[c]

[a] Università "Niccolò Cusano", via Don Carlo Gnocchi 3, Rome 00166, Italy
[b] School of Civil Engineering, The University of Sydney, Sydney, NSW 2006, Australia
[c] Dipartimento di Ingegneria Civile e Ingegneria Informatica, Università degli Studi di Roma Tor Vergata, Rome, Italy

ARTICLE INFO

*Article history:*
Revised 26 November 2018
Available online xxx

*Keywords:*
Crushing
Sand
Compressibility
Polydispersity

ABSTRACT

In this work we propose a micro to macro compressibility model to predict the deformation of soils with crushable grains subjected to one-dimensional compression loading. The grain size distribution of the media is described by a new index $I_G$ defining the degree of polydispersity. $I_G$ is linked to the evolution of the irreversible component of the deformation, while the reversible part is defined through the poroelasticity framework. The model is then applied to experimental data on monodisperse and polydisperse sand samples. Finally, this newly proposed compressibility model is coupled with an existing heterarchical multi-scale model that is able to represent how the grain size distribution evolves as a function of stress due to particle scale micromechanics. This combined heterarchical-compressibility model is shown to capture reasonably well the complex simultaneous interactions between the way the porosity, stress, and grain size distribution evolve for both initially monodisperse and polydisperse sands.



## 1. Introduction

Granular media such as sand, gravel and snow are common in both nature and industrial processes. Their mechanical behavior is affected by the intrinsic properties of individual grains, such as their shape and roughness, their chemical and physical composition and the grain size distribution. Experimental evidence indicates that grain size and shape are two important properties that influence the macroscopic density and mechanical behavior of the medium (Cubrinovski and Ishihara, 2002; Göncü and Luding, 2013; Santamarina and Cho, 2004), therefore playing a fundamental role in controlling soil deformation due to loading. These micro-scale features reflect the history of the material: its formation, transportation and deposition environments.

The concept of relative density gives an indication of how densely packed a material is compared to its intrinsic minimum and maximum values, which are practically determined using standard procedures as in ASTM-D4254 (2006). Determining these density limits precisely is an ongoing issue due to large uncertainties associated with their measurement and sensitivity of the test procedures (Oda, 1972; Youd, 1973). Density state is a result of the inter-particle network of forces generated, and of the nature of the interactions (Donev et al., 2005), mainly affected by grain stiffness, size, shape, and surface texture.

However, the fact that the minimum and maximum density are strongly correlated to the grain size distribution is experimentally well established: a monodisperse assembly – composed of particles with the same size – leads in general to a lower density state compared to a polydisperse one, since grains with a larger range of sizes can fill the inter-particle voids more efficiently. Therefore, the greater the range of sizes, the greater the density and the lower the minimum and maximum void ratios (*e.g.* Burmister, 1938; 1948; Cubrinovski and Ishihara, 2002; Miura et al., 1997; Nakata et al., 2001a; Peronius and Sweeting, 1985; Youd, 1973). Various experimental and theoretical studies describe bi-disperse packing, which highlight that in the presence of approximately 30% fines, the material reaches its maximum density (Cubrinovski and Ishihara, 2002; Dias et al., 2004; Farr and Groot, 2009; Lade et al., 1998; Wood and Maeda, 2008; Yu and Standish, 1988). Here, however, we are concerned with the more general problem of polydispersed materials.

In addition to the role of polydispersity, empirical evidence (Kolbuszewski and Frederick, 1963) shows that for monodisperse granular assemblies, the maximum and minimum densities tend to decrease with increasing particle size. This is attributed to a particle shape effect, where larger particles tend to be more rounded due to their formation via natural processes (Youd, 1973). Alternatively, this may be due to the effect of subtle surface forces, such as static electricity and adhesion (Miura et al., 1997).

* Corresponding author.
*E-mail addresses:* giulia.guida@unicusano.it (G. Guida), itai.einav@sydney.edu.au (I. Einav).

https://doi.org/10.1016/j.ijsolstr.2018.11.032
0020-7683/

Many authors have proposed empirical equations, based on a wide set of experimental data, to describe the increase of the minimum and maximum void ratio with a decrease of particle sphericity (*e.g.* Cho et al., 2006; Cubrinovski and Ishihara, 2002; Nakata et al., 2001a). Similar observations have been made for particle elongation, which was found (Fraser, 1935; Jia and Williams, 2001) to be inversely proportional to the packing density. Irregularity at all three morphological length scales – elongation (macro), angularity (meso) and texture (micro) – hinders particle mobility and thus inhibits the formation of denser assemblies.

Some researchers (*e.g.* Man et al., 2005; Ogarko et al., 2014; Torquato and Stillinger, 2010; Torquato et al., 2000) have investigated through simulations the upper and lower bound limits of density for hard spherical or even euclidean 3D shaped particles packing, and successfully reproduced prominent structural properties, especially at higher densities.

The density of a granular material, bounded between its intrinsic maximum and minimum values, reflects the physical state and the loading history of the medium: adopting standard procedures (ASTM-D4254, 2006) a dried pluviated material would have a density state close to its minimum value, while a vibrated or compacted material would have a density nearer its maximum value.

Under increasing stresses the tendency for particle crushing grows (*e.g.* Arshad et al., 2014; Wood and Maeda, 2008). The fragments produced can come in different shapes, while due to size reduction the degree of polydispersity generally increase. These factors affect the intrinsic physical properties of the material, not least the minimum and maximum density. The work in Rubin and Einav (2011), Tengattini et al. (2016) formulated the problem of maximum and minimum porosity evolution as a function of the amount of breakage, in terms of how the grain size distribution changes between its initial and assumed final state (Einav, 2007) using geometrical parameters related to particle shape and roughness (Cho et al., 2006). Recently, a micro-macro link has been established (Guida et al., 2018) between the evolution of the void ratio upon vertical loading, grain crushing and the evolution of the number of crushed particles, using X-ray tomography.

The prediction of porosity change due to loading is of fundamental importance in engineering mechanics, as well as in all related industrial processing because it affects the mechanical (strength and stiffness), hydraulic (permeability) and thermal (conductivity) properties of the overall material.

In the first part of this paper a compressibility model that links the porosity of the mixture to the grading polydispersity is developed in order to further contribute to bridging the gap between the micro structural properties and the macro mechanical behavior of a granular material. An index of grading $I_G$ is defined to describe the polydispersity and it is coupled to the evolution of the porosity due to loading by the newly proposed compressibility model. This model is then applied to experimental data and finally combined with a heterarchical crushing model (Marks and Einav, 2017) in order to predict both the grading evolution, and the resultant porosity changes. Using this last step, the current paper aims to establish an entirely complete compression model that couples the macroscopic stress-density relation to microscopic grain crushing mechanisms and statistical information of the evolving grainsize distribution.

## 2. Polydispersity

The dispersity of a set of particles is a measure of the heterogeneity of their sizes: a mixture of particles with the same size, shape and mass are termed uniform, or monodisperse, whilst a mixture with distributed properties is called non-uniform, or polydisperse. The full grain size distribution (GSD) of a soil can be determined experimentally by sieving and sedimentation methods (ASTM-D422-63, 2007; BS, 1990), or with advanced techniques such as master-sizer (Altuhafi et al., 2012; Sympatec, 2008) or image processing of three-dimensional images (Karatza et al., 2017). The GSD is usually presented as a cumulative curve (CGSD) on semi-logarithmic axes and is typically reported using descriptive indices such as $D_{50}$, the diameter of the particle which 50% of the mass is smaller than, and the coefficient of uniformity $C_u = D_{60}/D_{10}$, where $D_{60}$ and $D_{10}$ are the diameters which 60% and 10% of the mass are smaller than, respectively. Although these measures have historically been successfully applied to classify soils, particularly for separating well graded from poor graded soils, they are often not representative of the entire GSD (also known as the grading curve), because they are measures of one or two points on the distribution. As an example, Fig. 1 shows different artificial mixtures from (Youd, 1973) with varying polydispersity.

**Table 1**
Grain size distribution properties of five mixes of grains from (Youd, 1973).

| GSD properties | | | | | | | | |
|---|---|---|---|---|---|---|---|---|
| Mix | $d_{min}$ [mm] | $d_{max}$ [mm] | $\Delta d$ [mm] | $D_{50}$ [mm] | $C_u$ [-] | $I_{GS}$ [-] | $\bar{s}$ [-] | $I_G$ [-] |
| 1 | 0.50 | 0.95 | 0.45 | 0.63 | 1.4 | 0.05 | 0.71 | 1.08 |
| 2 | 0.25 | 1.88 | 1.63 | 0.25 | 2.5 | 0.14 | 0.37 | 1.40 |
| 3 | 0.12 | 3.72 | 3.60 | 0.09 | 4.3 | 0.21 | 0.15 | 2.14 |
| 4 | 0.08 | 5.04 | 4.96 | 0.05 | 8.0 | 0.24 | 0.10 | 2.72 |
| 5 | 0.13 | 1.91 | 1.78 | 0.28 | 4.3 | 0.15 | 0.31 | 1.65 |

The polydispersity grows from Mix 1, which is almost monodisperse, through Mixes 2 and 3, which are normally graded, to Mix 4 which is highly polydisperse. Mix 5, however, is a gap-graded distribution. The various grading indices of the GSD of Fig. 1, are reported in Table 1 in terms of $d_{min}$, $d_{max}$, $\Delta d = d_{max} - d_{min}$, $D_{50}$ and $C_u$. Mixes 3 and 5, even though qualitatively different, have the same $C_u$, because they intersect near $D_{10}$ and $D_{60}$. Furthermore, in cases where the percentage of fines is high and sieving measurements are limited, $D_{10}$ can often not be determined and $C_u$ cannot be evaluated.

The polydispersity of the GSD can also be evaluated through an integral method (Erguler, 2016), defining the grain size index $I_{GS}$ as the ratio between the area under the CGSD and the total area between 0.001 mm and $d_{max}$ (see corresponding values in Table 1). $I_{GS}$ assumes values bounded between 0 (monodisperse case) and 1 and it takes account of the slope, the shape and the position of the curve. It manages, unlike $C_u$, to recognize the difference between Mixes 3 and 5 (Fig. 1 and Table 1) giving to Mix 5 an index of grading in between Mix 2 and 3. However, this method works fine for a limited range of size and further the area under the grading curve does not always represent properly an index of polydispersity: *e.g.*, the $I_{GS}$ of a bi-disperse GSD, composed of a small amount of the large particles and a large amount of small particles, is close to 1, even if it would not be regarded as a polydisperse distribution.

In Göncü et al. (2010) and Kumar et al. (2014) further indices were proposed to faithfully represent the polydispersity of a 3D spherical system, based on moments of the grain size distribution. The work in this paper took inspiration by the concept of moment of sizes, but in the context of geotechnical experience, it focused on carrying only a single grading index based on the logarithm of the size distribution, as the interests are in the ratios between sizes, rather than size absolute value.

The grain size $d$ is non-dimensionalised with respect to the maximum grain size $d_{max}$ such that $s = d/d_{max}$. The use of $d_{max}$ rather than say $D_{50}$ ensures that $s$ is always between 0 and 1. It is possible to non-dimensionalise the grain size by any other size, however this makes the following grading index $I_G$ more difficult to interpret. Using this non-dimensional size, the geometric mean

Please cite this article as: G. Guida, I. Einav and B. Marks et al., Linking micro grainsize polydispersity to macro porosity, International Journal of Solids and Structures, https://doi.org/10.1016/j.ijsolstr.2018.11.032

$\bar{s}$ of the weight distribution is defined starting from its traditional formulation, $\bar{s} = \prod_i s_i^{w_i/w_{tot}}$, and then taking the natural logarithm of both sides, $\ln \bar{s} = \ln\left(\prod_i s_i^{w_i/w_{tot}}\right) = \sum_i \frac{w_i}{w_{tot}} \ln(s_i)$, such that:

$$\bar{s} = \exp\left[\sum_i \frac{w_i}{w_{tot}} \ln(s_i)\right], \tag{1}$$

where $w_i$ is the weight retained at the sieve opening $d_i$ and $w_{tot}$ is the total weight of the sample. This geometric mean captures the inherent advantages of the logarithmic scale for portraying the full details of grain size distributions, which often span across many log decades (Bagnold, 1953).

An index of polydispersity $I_G$, named the index of grading, is defined to overcome the limitations of the indices described above ($C_u$ and $I_{GS}$). $I_G$ is dimensionless, and is defined as the geometric standard deviation of the normalized set of sizes $s_i$. The geometric standard deviation describes the spread of GSD about a geometric mean $\bar{s}$ and is a direct analogy of the usual (arithmetic) standard deviation, but operating on log-scale data. This geometric standard deviation returns a value which is dimensionless and additionally preserves information related to smaller sizes.

$$I_G = \exp\sqrt{\sum_i \frac{w_i}{w_{tot}} (\ln s_i - \ln \bar{s})^2} = \exp\sqrt{\sum_i \frac{w_i}{w_{tot}} \ln^2\left(\frac{s_i}{\bar{s}}\right)}. \tag{2}$$

These definitions of $\bar{s}$ and $I_G$, as proposed in Eqs. 1 and 2 are compared with other measures in detail in Alderliesten (2005). The values of $\bar{s}$ and $I_G$ for the GSD shown in Fig. 1 are reported in the last two columns of Table 1. $I_G$ manages, better than $C_u$ to capture the difference between the gap-graded (Mix 5) and the graded mixture (Mix 3). Using this definition of the index of grading, Mix 5 has a polydispersity in between Mix 2 and Mix 3 (Fig. 1).

Another interesting formulation to describe GSD polydispersity is based on the concept of statistical entropy $S$ (Lőrincz et al., 2005):

$$S = -\sum_i w_i log_b(w_i), \tag{3}$$

where $b$ is the logarithmic base on which the GSD data is discretised. This formulation is very effective for describing degradation processes, stability and rates of breakage, but in order to characterize the polydispersity, a present limitation is that it is only defined in this discrete form and is dependent on the number of size fractions.

On the other hand, $I_G$ can be re-expressed using a continuum formulation, with integrals replacing the summations in Eq. (2) and $f(s)$ representing the smooth probability distribution function of the normalized grain sizes:

$$\begin{aligned} I_G &= \exp\sqrt{\int f(s) \ln^2\left(\frac{s}{\bar{s}}\right) ds}, \\ \bar{s} &= \exp\left[\int f(s) \ln(s) ds\right]. \end{aligned} \tag{4}$$

The index of grading $I_G$ is formally bound between 1, for a perfectly monodisperse case (as is $C_u$) and infinity, for an extremely polydisperse case. To better understand the upper bound limits of $I_G$, several artificial power law grain size distributions are analyzed and shown in Fig. 2. They are produced using the power law cumulative distribution function with minimum and maximum cutoffs (see (Einav, 2007)):

$$F(d) = \frac{d^{3-\beta} - d_{min}^{3-\beta}}{d_{max}^{3-\beta} - d_{min}^{3-\beta}}, \tag{5}$$

where $\beta$ is the power law dimension of the grading curve (often referred to as the fractal dimension). In the limit where $d_{\min} = 0$,

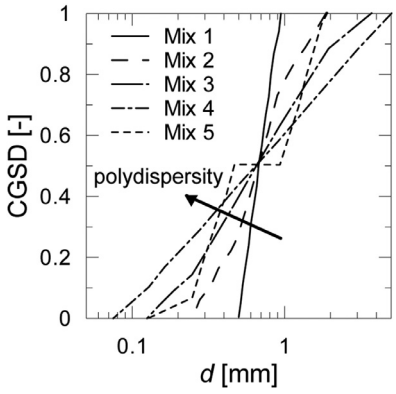


**Fig. 1.** Cumulative grain size distribution (CGSD) of mixes 1–5 reproduced from (Youd, 1973).

the relationship above reduces to the traditional power law formulation $F(d) = \left(d/d_{\max}\right)^{3-\beta}$. Fig. 2a-b show six power law grading functions on semi-logarithmic and linear axes respectively, characterized by six different values of $\beta$: from $\beta = -5$, corresponding to an almost monodisperse case, to a value tending to 3. In each case, $d_{\min} = 0.001$ mm and $d_{\max} = 1$ mm.

Figs. 2c and d show the trend of $I_G$ and $\bar{s}$, $C_u$ and $D_{50}$ as functions of the exponent $\beta$. The trend of the derivatives, $dI_G/d\beta$ and $dC_u/d\beta$, are also reported in Figs. 2c and d respectively. Both indices start to increase significantly from $\beta \approx 1$, monotonically in the case of $I_G$ and with a peak on $\beta \approx 2.8$ for $C_u$. The maximum values of $I_G$ and $C_u$ increase as the minimum size $s_{\min} = d_{\min}/d_{\max}$ decreases, and when $s_{\min} = 0$, $I_G$ tends to infinity.

The major difference between $I_G$ and $C_u$ are due to the scales of the definitions: logarithmic for $I_G$ (Fig. 2a) and linear for $C_u$ (Fig. 2b). Considering Fig. 2a, the CGSD with $\beta = 2.999$ appears undoubtedly more polydisperse than the one with $\beta = 2.5$, while for Fig. 2b the opposite is true. Computing $C_u$ in a logarithmic space, as $\ln(D_{60})/\ln(D_{10})$, its trend with $\beta$ increases monotonically, as for $I_G$.

Fig. 3 reports the maximum and minimum porosity values, respectively $\phi_{\max}$ and $\phi_{\min}$, as a function of the index of grading $I_G$ and $\bar{s}$, for two different classes of sand, with GSD (Mix 1–5) of Fig. 1, as measured in Youd (1973).

The analyzed sands, MOL and CB, are both artificially assembled: the first, MOL, is a mix of Monterey, Ottawa, Lapis Lustre and Del Monte sands, while the second, CB, is Crushed Basalt. These two granular materials are characterized by different grain morphology, respectively sub-rounded and angular, according to the classification of Powers (1953).

Figs. 3a and b shows a decreasing trend of $\phi_{\max}$ and $\phi_{\min}$ with $I_G$, and a increasing trend with $\bar{s}$, regardless of the material. The increase of polydispersity is directly associated with a decrease of $\bar{s}$, which indicates how far the average size is from the maximum diameter (see Fig. 2), and leads directly to denser states due to the increased packing ability of the grains. The influence of the different particle morphologies is observed in the magnitude of the porosity values: MOL mixtures, being more rounded and regular, present systematically lower porosity values than CB mixtures, that instead are characterized by more angular and irregular particles. As described above, this occurs because rounded and regular grains are more free to rearrange due to the lower surface friction and geometrical resistance to rolling.

## 3. Micro to macro compressibility model

The compressibility of granular materials is affected by density (or porosity) and by the state of the effective stress. Grain crushing

Please cite this article as: G. Guida, I. Einav and B. Marks et al., Linking micro grainsize polydispersity to macro porosity, International Journal of Solids and Structures, https://doi.org/10.1016/j.ijsolstr.2018.11.032

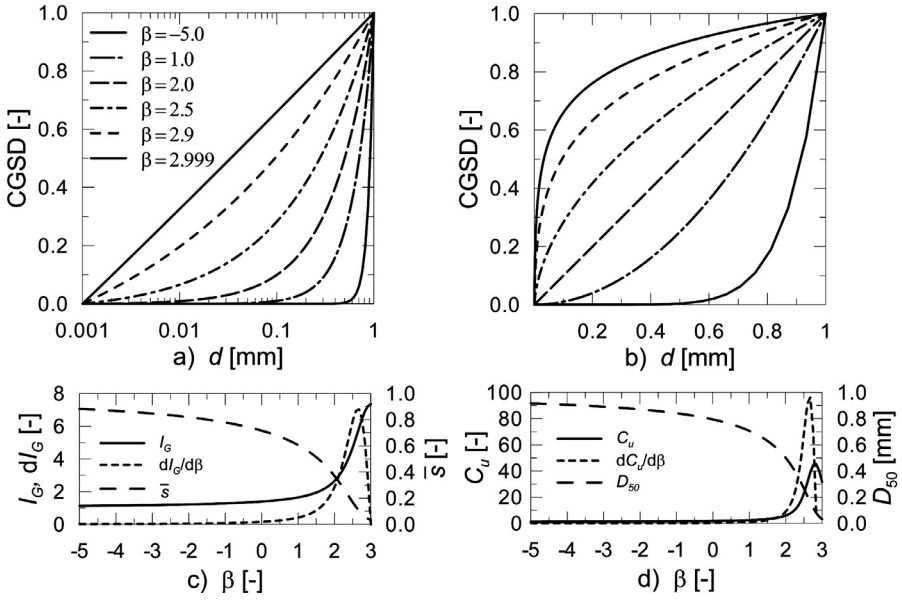


**Fig. 2.** Power-law CGSD for varying $\beta$ in: a) semi-logarithmic scale; and b) linear scale, respectively. Variations of indices with corresponding $\beta$ values: c) variation of $I_G$, $dI_G/d\beta$ and $\bar{s}$; and d) variation of $C_u$, $dC_u/d\beta$ and $D_{50}$.

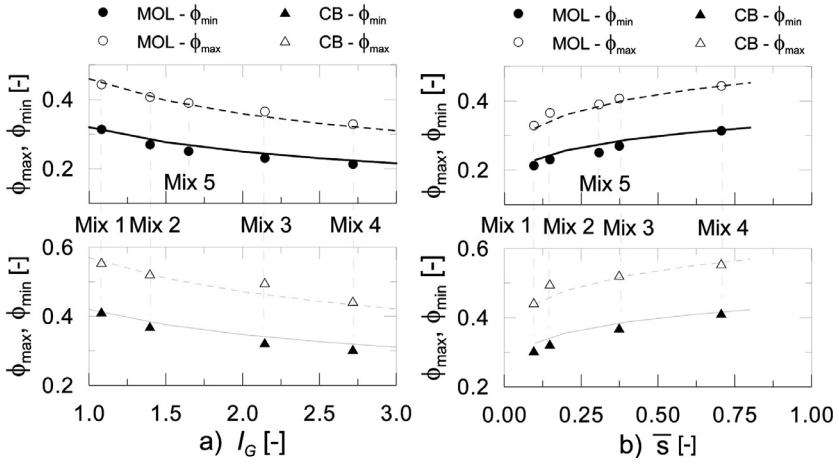


**Fig. 3.** Variations of the maximum and minimum porosities with a) $I_G$ and b) $\bar{s}$ for the two different sands of Youd (1973): MOL (top) and CB (bottom). The mixtures shown (Mix 1–5) are the same as in Fig. 1. Solid lines represent best fits using Eq. (12) with $\phi_{min}^{MONO}$ =0.33, $\phi_{max}^{MONO}$ =0.46, and $\alpha$=0.36 for MOL and $\phi_{min}^{MONO}$ =0.43, $\phi_{max}^{MONO}$ =0.57 and $\alpha$=0.28 for CB.

modifies the size distribution and the shape of the grains, affecting consequently the state of density of the material. The prediction of deformation induced by loading and grain crushing represents a fundamental step forward in the micro-macro mechanical modeling of granular materials. In this work, following the approach proposed by Tengattini et al. (2016), the volumetric increment of deformation $\dot{\epsilon_v}$ is split into two contributions, one due to the deformation of the solid phase $V_s$, and the other linked to porosity $\phi$ and its rate of change $\dot{\phi}$, as:

$$\dot{\epsilon_v} = -\frac{\dot{V_s}}{V_s} - \frac{\dot{\phi}}{1-\phi}, \tag{6}$$

which follows from the definition of the total volumetric strain rate ($\dot{\epsilon_v} = -\dot{V_t}/V_t$, the change of the total volume over the original total volume). Assuming that the solid phase is incompressible, $\dot{V_s} = 0$, the compressibility of the material can be directly modeled using the total porosity rate $\dot{\phi}$ (see Eq. (7)) that involves both reversible $\dot{\phi}_{el}$ and irreversible $\dot{\phi}_{pl}$ contributions as:

$$\dot{\phi} = \dot{\phi}_{el} + \dot{\phi}_{pl}, \tag{7}$$

with $\dot{\phi}_{el}$ linked to the inter-granular elastic strains of the material, and $\dot{\phi}_{pl}$ to particle rearrangement, which is enhanced by grading changes. As a first step, the model is formulated under one-dimensional conditions, which is able to reproduce the lithostatic conditions of granular materials.

### 3.1. Elastic component

The elastic behavior of the soil skeleton is described in the framework of poroelasticity, which is firmly based on a micro-mechanical approach (Detournay and Cheng, 1994). The reversible volumetric response of a porous material is linked to the change in pressure $\sigma$ as the sum of two terms:

$$\frac{\dot{\phi}_{el}}{(1-\phi)} = -\frac{\dot{\sigma}}{K_s} - \frac{\dot{\sigma}}{K_\phi}, \tag{8}$$

where $K_s$ and $K_\phi$ are the bulk moduli of the solid phase and of the porous solid, respectively, while $-\dot{\sigma}/K_s$ and $-\dot{\sigma}/K_\phi$ their relative deformation rates. The compressibility of the solid phase can

Please cite this article as: G. Guida, I. Einav and B. Marks et al., Linking micro grainsize polydispersity to macro porosity, International Journal of Solids and Structures, https://doi.org/10.1016/j.ijsolstr.2018.11.032

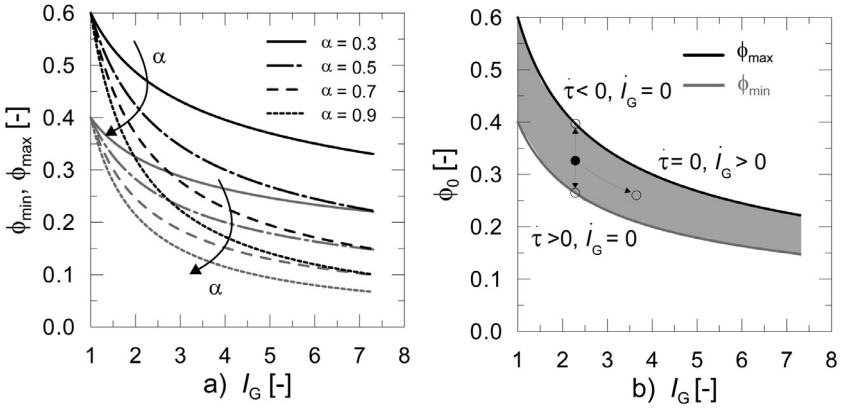


**Fig. 4.** a) Evolution of $\phi_{\min}$ and $\phi_{\max}$ with grain crushing expressed by $I_G$ of Eq. (12), for different values of $\alpha = 0.3 - 0.9$; b) possible scenarios of unstressed porosity, $\phi_0$ changes inside the band limited by $\phi_{\min}$ and $\phi_{\max}$.

be assumed negligible compared to that of the drained bulk material, because $K_s \gg K_\phi$. Furthermore, assuming that the pores are spherical and in an isotropic loading condition (Mackenzie, 1950), it has been shown that:

$$K_\phi = \frac{4G}{3\phi}(1-\phi), \tag{9}$$

where $G$ is the shear modulus of the soil and $\phi$ the global porosity state variable. In the limit where the porosity $\phi \to 0$, $K_\phi \to \infty$ (according to Eq. 9), the elastic component of deformation is just related to the deformability of the solid phase.

It is noted that the stiffness of the porous solid does not depend on the stiffness of the solid phase, but only on the shear stiffness of the porous material, related to the frictional contacts between grains. $G$ itself, however, is strongly affected by the mean effective confining pressure and porosity of the medium (Senetakis et al., 2012; Viggiani and Atkinson, 1995). To capture these effects, an empirical formulation (Rubin and Einav, 2011) was adopted:

$$G = g(1-\phi)^{\frac{3}{2}}\left(\frac{\sigma}{\sigma_a}\right)^{\frac{1}{2}}, \tag{10}$$

where $\sigma_a$ is the atmospheric pressure and $g$ is a dimensional stress parameter [F/L$^2$] that is required to be calibrated by experiments. The shear modulus is expected to increase with decreasing $\phi$ and increasing confining stress $\sigma$.

### 3.2. Plastic component

We start by defining an unstressed porosity $\phi_0$, a property consistent with the methods (ASTM-D4254, 2006) of measuring the limiting porosities $\phi_{\max}$ and $\phi_{\min}$ under zero stress:

$$\phi_0 = \tau\phi_{min} + (1-\tau)\phi_{max}, \tag{11}$$

where $\tau$ is the auxiliary porosity index (Rubin and Einav, 2011; Tengattini et al., 2016). When $\tau = 1$, $\phi_0 = \phi_{\min}$ and when $\tau = 0$, $\phi_0 = \phi_{\max}$. The values of $\phi_{\min}$ and $\phi_{\max}$ depend on both the GSD and the particle shape (Althuhafi and Coop, 2011), as shown in Fig. 1a. The following power law functions between $\phi_{min/max}$ and the index of grading $I_G$ are assumed:

$$\begin{aligned} \phi_{min} &= \phi_{min}^{MONO} I_G^{-\alpha}, \\ \phi_{max} &= \phi_{max}^{MONO} I_G^{-\alpha}, \end{aligned} \tag{12}$$

where the two constants $\phi_{\min}^{MONO}$ and $\phi_{\max}^{MONO}$ are the minimum and maximum porosities at zero stress of a monodisperse grading (when $I_G = 1$) and $\alpha$ is a dimensionless model parameter dependent on grain properties. The above relationship describes the decrease of porosity as polydispersity increases consistently with other experimental and numerical findings (Kumar et al., 2014; Nakata et al., 2001b; Ogarko and Luding, 2013; Youd, 1973). Note that in Eq. 12, the effect of grain shape is only captured in $\phi_{\min}^{MONO}$ and $\phi_{\max}^{MONO}$, while the effect of changing particle shape on the evolution of $\phi_{\min}$ and $\phi_{\max}$ is ignored.

Taking the rate of change of the unstressed porosity (11), we obtain:

$$\dot{\phi}_0 = \left[\tau\dot{\phi}_{min} + (1-\tau)\dot{\phi}_{max}\right] + (\phi_{min} - \phi_{max})\dot{\tau}. \tag{13}$$

In predominantly compressional loading, the auxiliary index $\tau$ is assumed not to vary during loading ($\dot{\tau} = 0$), and the plastic strain rate could be evaluated by the rate of change of the unstressed porosity, only depending by the rate of change of $\phi_{\max}$ and $\phi_{\min}$, thus by the evolution of grading polydispersity due to grain crushing:

$$\dot{\phi}_{pl} \approx \tau\dot{\phi}_{min} + (1-\tau)\dot{\phi}_{max}. \tag{14}$$

In a more general loading condition, the rate of change of the plastic porosity would have to be extended to capture grain rearrangement phenomena associated with granular temperature such as *e.g.* dilation.

As shown in Fig. 3, this model for the unstressed porosity evolution is reasonable. The main difference between the curves could be attributed to grain morphology, being sub-rounded and angular respectively. In these two samples, the increased irregularity of grain shape led of course to greater $\phi_{min/max}^{MONO}$ and also to a lower value of $\alpha$.

Fig. 4a shows the evolution of $\phi_{\min}$ and $\phi_{\max}$ as a function of $I_G$, with $\phi_{\min}^{MONO} = 0.4$ and $\phi_{\max}^{MONO} = 0.6$, for various values of $\alpha$. Lower values of $\alpha$ correspond to a less compressible behaviour, *i.e.* a smaller change in $\phi$ for a given change in $I_G$. Fig. 4b shows possible variations of the unstressed porosity, $\phi_0$. Recall that in this work a constant $\tau$ is assumed and thus follow the indicated $\dot{\tau} = 0$ line in this figure.

## 4. Application to crushable granular soil

In Nakata et al. (2001a) and Nakata et al. (2001b), one-dimensional compression tests for both initially monodisperse (diameters ranging between 1.4 mm and 1.7 mm) and polydisperse (diameters ranging between 0.25 mm and 2.0 mm) samples are performed, and their grading curves are shown in Fig. 5a and b as a function of vertical stress. The compressibility model proposed above is applied to this data in Fig. 5c to examine the evolution of $I_G$ in relation to yielding. It is evident that yielding in terms of grain crushing for the monodisperse case begins earlier than for the polydisperse case, since its grading changes more rapidly at lower stress.

Please cite this article as: G. Guida, I. Einav and B. Marks et al., Linking micro grainsize polydispersity to macro porosity, International Journal of Solids and Structures, https://doi.org/10.1016/j.ijsolstr.2018.11.032

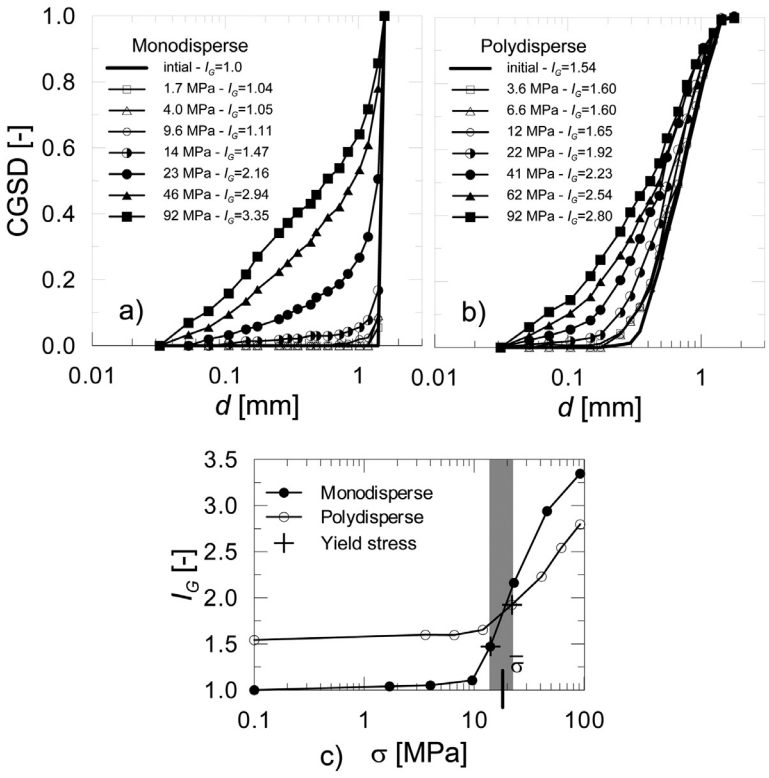


**Fig. 5.** Grading curve evolution with increasing vertical loading for a) initially monodisperse GSD and for b) initially polydisperse GSD taken from Nakata et al. (2001a). c) Evolution of $I_G$ with vertical stress for both cases. 'Yielding', as indicated in gray, may be associated with a sharp variation in $I_G$, although we note that it is actually a continuous process, with grain crushing observable at nearly any stress level.

**Table 2**
Complete set of the macro-scale parameters the silica sand used in Nakata et al. (2001a) required for the compressibility model. Note that the above model depends on only one parameter with dimensions ($g$), with it all other parameters being purely geometrical.

| Monodisperse | | | | Polydisperse | | | | | |
|---|---|---|---|---|---|---|---|---|---|
| $\phi_{\min}^{MONO}$ | $\phi_{\max}^{MONO}$ | $\phi_i$ | $\tau$ | $\phi_{\min}^{MONO}$ | $\phi_{\max}^{MONO}$ | $\phi_i$ | $\tau$ | $\alpha$ | $g$ |
| [-] | [-] | [-] | [-] | [-] | [-] | [-] | [-] | [-] | [MPa] |
| 0.38 | 0.47 | 0.39 | 0.8 | 0.41 | 0.52 | 0.36 | 0.1 | 0.3;0.5;0.8 | 175 |

Table 2summarizes all of the macro scale parameters needed for the calibration of the compressibility model against experimental data. Note that $\phi_{\min}^{MONO}$ and $\phi_{\max}^{MONO}$ are deduced by Nakata et al. (2001b). As described above, also note that these values are a function of grain shape, which are different for the two gradings studied. For consistency and simplicity, the reported values are chosen for the initial smallest grains in each sample.

The monodisperse sample is prepared in a relatively dense state, while the polydisperse case corresponds to a relatively loose state, as shown in the Table 2. In the following the effect of varying $\alpha$ on the compressibility is examined, as $\alpha$ is the only free parameter.

Finally, the elastic contribution of the porosity evolution is calibrated in accordance with Eq. (10). The parameter $g$ is obtained by fitting the small strain shear stiffness measurements on natural quartz sand (Senetakis et al., 2012) as a function of the effective stress and porosity, as shown in Fig. 6.

According to the compressibility model of Section 3, for each loading stage $k$ at which the GSD and stress level are known, the total porosity $\phi^k$, is computed as the sum of the porosity of the previous stage plus an increment $\Delta\phi^k < 0$ (negative in 1D compression) , composed of elastic $\Delta\phi_{el}^k$ and plastic $\Delta\phi_{pl}^k$ parts.

$$\begin{aligned} \phi^k &= \phi^{k-1} + \Delta\phi^k, \\ \Delta\phi^k &= \Delta\phi_{el}^k + \Delta\phi_{pl}^k < 0. \end{aligned} \tag{15}$$

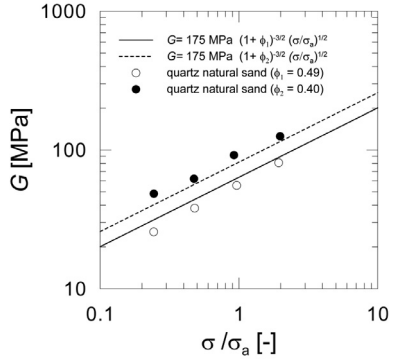


**Fig. 6.** Calibration of the parameter $g$ from the experimental data of Senetakis et al. (2012).

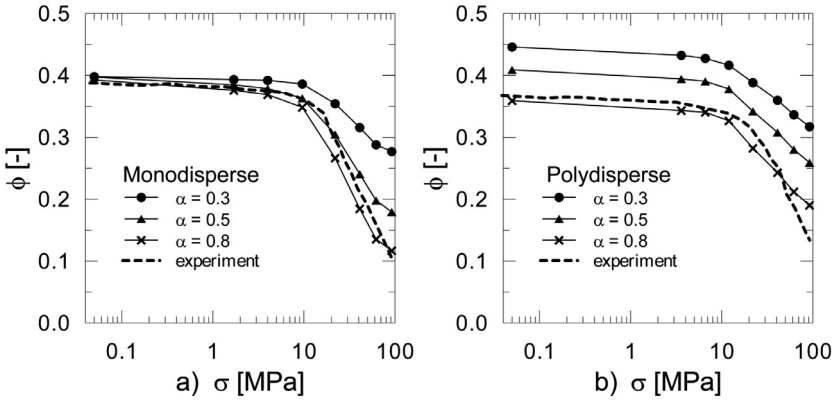


**Fig. 7.** Theoretical and experimental (Nakata et al. (2001a) and Nakata et al. (2001b)) porosities over vertical stress for a) initially monodisperse and b) initially polydisperse samples during one-dimensional compression for various values of $\alpha$.

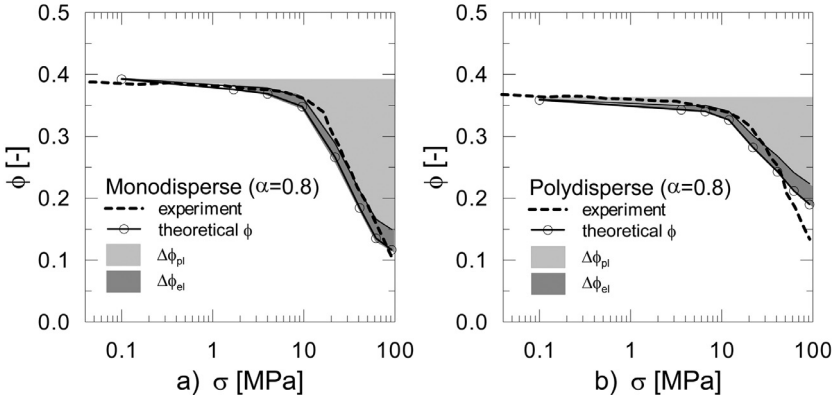


**Fig. 8.** Re-examining Fig. 7 for $\alpha = 0.8$ for initially a) monodisperse and b) polydisperse samples, with cumulative porosity changes being separated for the plastic (light grey area) and the elastic contributions (dark grey area).

The variation of the elastic part is computed based on Eq. (8) as:

$$\Delta\phi_{el}^{k} = -\frac{\Delta P^{k}}{K_{\phi}^{(k-1)}} < 0, \tag{16}$$

where $K_\phi$ depends on the total porosity $\phi$ at the previous loading stage $k-1$. The increment of the plastic part $\Delta\phi_{pl}^{k}$ is simply calculated from the difference of the state of the unstressed porosities as:

$$\Delta\phi_{pl}^{k} = \phi_0^{k} - \phi_0^{k-1} < 0. \tag{17}$$

Fig. 7 shows the evolution of porosity with loading for initially monodisperse (Fig. 7a) and polydisperse (Fig. 7b) samples during one-dimensional compression tests up to 92 MPa. Experimental measurements (Nakata et al., 2001a; 2001b) are compared with the model results evaluated at the loading stages corresponding to the known GSD (corresponding to symbols on Fig. 7) for three values of $\alpha$.

The model can replicate quite well the apparent yield point and the pre- and post-yield evolution of the porosity. As the polydisperse corresponds to $I_G$ different than unity, its initial porosity depends on the choice of $\alpha$. The $\alpha = 0.8$ curve best fits the experimental data, which represents angular and irregular particles.

Fig. 8 re-examines these experimental and model lines for the $\alpha = 0.8$ case, in terms of the split between the elastic and plastic cumulative changes of the porosities from the start of the tests, highlighted separately. Starting from the apparent yield point, most of the porosity variation comes from the plastic contribution related to the grain crushing phenomena. On the other hand, the elastic contribution controls the compressibility pre-yield, and could also give an indication of the swelling behavior of the sample during unloading, after crushing, if experimental data were available to compare with.

## 5. Micro to macro crushing-compressibility model

In the previous sections a micro to macro compressibility model was developed and tested, which connects macroscopic stress and porosity to the microstructural state of the grain size distribution. The remaining question is, how to predict this microstructural state. Here, the use of the "heterarchical model" in Marks and Einav (2011, 2015, 2017) resolves this critical point.

Unlike earlier models that represent the grain-size distribution using a single scalar breakage variable *e.g.*, (Einav, 2007; Hardin, 1985), the heterarchical model depends on the whole GSD with grain crushing developing stochastically at a microstructural grain scale. In this model a regular $(N+1)$-dimensional lattice is defined, with $N$ being the number of spatial coordinates and the $+1$ representing the additional microstructural coordinate which preserves information at a finer resolution below the representative volume element about the microscopic grainsize and nearest neighbours' grainsize. Each cell of the lattice is related to a certain physical position in space and to a determined mass fraction of a particle size of the grading (see Marks and Einav (2015, 2017) for more details).

Here, we explore the constitutive response of only a single macroscopic point in space *i*. In other words, we make use of only the single $+1$ microstructural coordinate. Nevertheless, we wish to emphasize that the possible use of the $N$ dimensional model is

conceptually important, as it can allow us to couple in the future the full constitutive process of the grain crushing phenomenon with possible grainsize mixing and segregation that can occur in open systems (Marks and Einav, 2015; 2017).

In this model grain crushing develops only if the applied stress in the i$^{th}$ microstructural lattice cell, $\sigma_i^t$, exceeds its crushing critical value, $\sigma_i^c$:

$$if \quad \sigma_i^t \geq \sigma_i^c \quad \rightarrow \quad \text{crushing.} \tag{18}$$

The microstructurally local tensile stress, $\sigma_i^t$, is found by mapping the externally applied stress, $\sigma^t$, in a way that considers the effects of neighbours' cushioning (see Appendix). This cushioning factor is taken such that when particles are surrounded by neighbours of the same size, the local tensile stress is equal to the bulk one, yet the stress goes to zero when the neighbours are far from the same size (Marks and Einav, 2017).

The strength, $\sigma_i^c$, in the microstructural i$^{th}$ cell is drawn from a size-dependent Weibull distribution (Ben-Nun and Einav, 2010; McDowell and Bolton, 1998), with bigger grains being weaker due to increasing chance for imperfections within the grains (Weibull, 1939). When grain crushing occurs, the grain size in that cell is updated by drawing a new size from an imposed fragment size distribution. The particle strength as well, associated to the size, is updated every time the breakage phenomenon takes place.

### 5.1. Results

The one-dimensional compression tests on monodisperse and polydisperse (Nakata et al., 2001a), as already reported in Section 4, are here simulated using the combination of the compressibility and heterarchical models, with the former predicting the dependence of the porosity on the GSD and the latter predicting how the GSD evolves as a function of the stress. The details on the implementation of this merged model (open source code provided in Marks and Guida (2018)) and on the calibration procedure used to determine the parameters are reported in the Appendix.

Fig. 9a shows how the combined compressibility-heterarchical model predicts the experimental results in terms of compressibility (porosity $\phi$ against vertical stress $\sigma$) for monodisperse and polydisperse samples. The model predicts qualitatively well the experimental behaviour over the whole range of stress investigated, from pre- to post-yielding. It also predicts quantitatively well the polydisperse case. However, the monodisperse case is slightly underestimated by the model with the point of yield reached at a lower stress than the experiment, with grain crushing beginning too early in the heterarchical crushing model. This may be attributed to the possible different effect of cushioning (see Appendix) assumed the same for the two cases. Finally, though there is no experimental data to compare with for this set of comparisons, the model shows a very reasonable elastic unloading, here starting in both cases from $\sigma_{\max} = 92$ MPa.

Figs. 9b and c evaluates how the model predicts the experimental data of the cumulative grain size distributions (CGSDs). Accordingly, the heterarchical model predicts quantitatively fairly well the evolution of the CGSD under increasing vertical stress. However, for the initially monodisperse case (Fig. 9b) the qualitative comparison is generally only fair, though the shape of the lines for the smaller grain sizes is predicted rather nicely. The apparent discontinuity of the modelled CGSD at around $s \approx 1$ may be partly reasoned by continuous grinding of larger grains' asperities in the experiments, which is not taken into account through the model. Note that calculations are carried out with fragmentation probability function that follows either Weibull, power law or uniform distributions. While these affect the shape of the CGSD, especially at first stages, this effect is not that significant, and thus cannot probably reason the above mentioned discontinuity. Finally, we note that the model agrees with the experimental finding that the initially monodisperse sample experiences larger overall variations from the initial CGSD compared to the polydisperse samples.

## 6. Conclusion

This paper presents a simple micro to macro compression model for granular materials whose macroscopic stress response is driven by microstructural stochastic phenomena of grain crushing using a heterarchical approach that allows to calculate the evolving grain size distribution, itself controlling the macroscopic "unstressed" porosity. The latter property is bounded by maximum and minimum porosities at zero stress per usual protocols (ASTM-D4254, 2006). Changes to the unstressed porosity lead to changes in irreversible plastic porosity, while the reversible elastic porosity is calculated using the continuum poroelasticity theory. In return, overall porosity changes are recovered by summing up these irreversible and reversible contributions. The relation for the unstressed macroscopic porosity in terms of the grain size distribution is motivated experimentally, using a single newly defined index of grading $I_G$, the geometric standard deviation of grain size distribution. It is inspired by the definition of the first two-order logarithmic moments of size distribution, sufficient for the current paper to properly characterize the dispersion of grainsize.

The compressibility model was successfully applied to experimental data of high pressure one-dimensional compression tests (Nakata et al., 2001a) which involves substantial grain crushing. Most of the variation in the porosity is shown to be due to its irreversible component, which indeed increases due to increasing polydispersity upon continuous grain crushing. On the other hand, the elastic contribution shows to control the compressibility prior to apparent yield, which marks the stress level at which significant grain crushing occur.

The irreversible variation of porosity is here assumed to be in such a way that the material relative density remains constant during the tests, which is thought to be realistic for predominantly compressional tests. This assumption may require alteration for tests involving substantial shear, where grains significantly dilate, or during vibration, where granular temperature may change the relative density even without changing the stress.

Further future considerations should be paid to relaxing some other simplifying steps. For example, the effect of grain morphology is here only taken through the initial values of the minimum and maximum densities, which change only as a function of grain size. However, grain morphology could also obviously change during loading, with initially spherical grains becoming more angular, and conversely, extremely angular grains becoming rounder. Extensions might be required to introduce new independent morphological state variables, potentially even in terms of new probability distributions. However, since the grain size may be considered as the first and simplest indicator of grain morphology, all other indicators might come with the cost of unwanted complexity. How to tackle this problem is an open question. As another example, the rules which dictate the progression of grain crushing using the heterarchical model may also be extended to include grain-size dependent grinding processes, which may smooth any discontinuity in the grain size distribution for initially monodisperse samples.

In summary, the current work establishes both a unique new opportunity for interpreting experimental data, as well as a way for predicting a variety of engineering soil properties such as permeability and retention features that are strongly dependent on the grain size distribution. The bonus of this particular model is in its ability to both predict how the porosity changes with stress, and these two variables change (or affect) the grain size distribution.

Please cite this article as: G. Guida, I. Einav and B. Marks et al., Linking micro grainsize polydispersity to macro porosity, International Journal of Solids and Structures, https://doi.org/10.1016/j.ijsolstr.2018.11.032

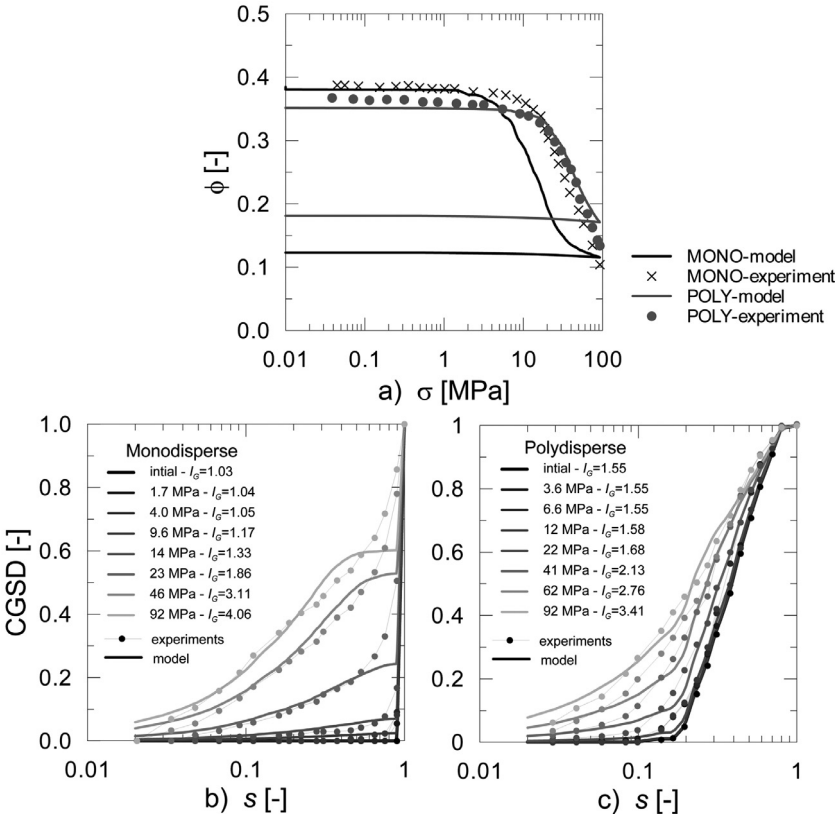


**Fig. 9.** a) Model prediction and experimental data (from Nakata et al. (2001a)) of the porosity $\phi$ plotted against the vertical stress $\sigma$ for both initially monodisperse (MONO) and polydisperse (POLY) grain size distributions. Experimental and simulated cumulative grain size distributions (CGSDs) for initially b) monodisperse and c) polydisperse samples.

## Appendix A

*Heterarchical model: calibration and analysis*

Apart from the initial grain size distribution, five additional parameters are required for the definition of the heterarchical model:

- Parameters defining particle strength, such as the critical reference strength, $\sigma_0^c$ and the Weibull modulus, $w$. Here the strength of each cell, $\sigma_i^c$, is drown from a Weibull distribution (McDowell and Bolton, 1998; Ben-Nun and Einav, 2010):

$$P(s_i) = \exp\left[-\left(\frac{s_i}{s_0}\right)^3\left(\frac{\sigma_i^c}{\sigma_0^c}\right)^w\right], \tag{19}$$

  where $P(s_i)$ is the crushing probability of a particle with normalized size $s_i = d_i/d_{\max}$ when loaded with an applied stress of $\sigma_0^c$ relative to a the critical strength of a reference particle with size $s_0$. $\sigma_0^c$, which corresponds to the stress at which the 37% of particles of size $s_0$ are survived, and $w$ is the Weibull modulus calibrated against experimental results.
- Parameters describing the fragment size distribution, $\kappa$ and $\lambda$. Here, a normalized two-parameter Weibull distribution function (Cheong et al., 2004; Marks and Einav, 2017) is used, which represents the probability of creating particles of size $s$ given the crushing of particles of size $s'$.

$$P(s|s') = \frac{\frac{\kappa}{\lambda}\left(\frac{s}{\lambda s'}\right)^{\kappa-1} e^{-\left(\frac{s}{\lambda s'}\right)^{\kappa}}}{1 - e^{-\left(\frac{1}{\lambda s'}\right)^{\kappa}}}, \tag{20}$$

  where $\kappa$, and $\lambda$ are parameters controlling respectively the assortment and the average size of the fragments.

**Table 3**
Micro scale parameters of a Silica sand used for the heterarchical crushing model. $\sigma_0^c$ is evaluated at a reference size $d_0 = 1.55$ mm.

| lattice size | | grain strength | | fragments size distr. | | cushioning |
|---|---|---|---|---|---|---|
| #$i$ | #$j$ | $\sigma_0^c$ [MPa] | $w$ [-] | $\kappa$ [-] | $\lambda$ [-] | $n$ [-] |
| 10 000 | 1 | 30.96 | 3.04 | 1.0 | 0.5 | 0.5 |

- The effect determining how strongly neighbours provide cushioning, in terms of the parameter $n$. This parameter comes in the scaling factor, $\zeta_i$, that relates the external applied stress to the local stress through the relation

$$\sigma_i^t = \sigma^t \zeta_i. \tag{21}$$

  This scaling is such that when particles are surrounded by neighbors of the same size, the local tensile stress is equal to the bulk one, and this stress goes to zero when the neighbours are far from the same size (Marks and Einav, 2017).

$$\zeta_i = \exp\left[-\frac{\ln(\frac{s_i}{\bar{s}_i})}{2n^2}\right], \tag{22}$$

  where $\bar{s}_i$ is the mean size of cell neighbors.

Table 3 summarizes the stochastic heterarchical lattice model parameters used for the sand samples of (Nakata et al., 2001a) that are used identically for both the monodisperse and polydisperse samples. The lattice has 10,000 cells for the internal coordinate $i$ (thus ensuring statistical representativeness), and one cell to the physical coordinate $j$, assuming as unique reference coordinate for the physical volume. The strength parameters are calculated from reported values provided in Nakata et al. (2001b) corresponding to a reference size $d_0$ =1.55 mm. The fragment size distributions

and $\kappa$, $\lambda$ and $n$ are calibrated by trial and error to give the best agreements in term of GSD evolution.

The numerical implementation of the merged model is given in an open source code, (Marks and Guida, 2018), which follows three key steps:

- Computation of the index of grading $I_G$ from the values $s_i$ of each cell;
- Evaluation of porosity variation $\Delta\phi$ during loading, as a superimposition of the elastic and the plastic components;
- Evaluation of the compressibility curve.

## References

Alderliesten, M., 2005. Mean particle diameters. from statistical definition to physical understanding. J. Biopharm. Stat. 15 (2), 295–325.
Althuhafi, F., Coop, M., 2011. Changes to particle characteristics associated with the compression of sands. Géotechnique 61 (6), 459–471.
Altuhafi, F., Osullivan, C., Cavarretta, I., 2012. Analysis of an image-based method to quantify the size and shape of sand particles. J. Geotech. Geoenviron. Eng. 139 (8), 1290–1307.
Arshad, M., Tehrani, F., Prezzi, M., Salgado, R., 2014. Experimental study of cone penetration in silica sand using digital image correlation. Géotechnique 64 (7), 551–569.
ASTM-D422-63, S., 2007. Standard test method for particle-size analysis of soils.
ASTM-D4254, S., 2006. Standard test methods for minimum index density and unit weight of soils and calculation of relative density.
Bagnold, R.A., 1953. The physics of blown sand and desert dunes. Methuen.
Ben-Nun, O., Einav, I., 2010. The role of self-organization during confined comminution of granular materials. Philosophical Transactions of the Royal Society A: Mathematical, Physical and Engineering Sciences 368 (1910), 231–247.
BS, 1990. Soils for civil engineering-part 2. British standard 1377-2.
Burmister, D.M., 1938. The grading-density relations of granular materials. American Society for Testing Materials.
Burmister, D.M., 1948. The importance and practical use of relative density in soil mechanics. In: Proceedings-American Society for Testing and Materials, 48, pp. 1249–1268.
Cheong, Y., Reynolds, G., Salman, A., Hounslow, M., 2004. Modelling fragment size distribution using two-parameter Weibull equation. Int. J. Miner. Process. 74, S227–S237.
Cho, G., Dodds, J., Santamarina, J.C., 2006. Particle shape effects on packing density , stiffness , and strength : natural and crushed sands. J. Geotechn. Geoenviron.Eng. 5 (132), 591–602.
Cubrinovski, M., Ishihara, K., 2002. Maximum and minimum void ratio characteristics of sands. Soils and Foundations 42 (6), 65–78.
Detournay, E., Cheng, A.H., 1994. Fundamentals of poroelasticity. Int. J. Rock Mech. Min. Sci. Geomech. Abstr. 31 (3), 138–139.
Dias, R.P., Teixeira, J.A., Mota, M.G., Yelshin, A.I., 2004. Particulate binary mixtures: dependence of packing porosity on particle size ratio. Indust.Eng.Chem.Res. 43 (24), 7912–7919.
Donev, A., Torquato, S., Stillinger, F.H., 2005. Pair correlation function characteristics of nearly jammed disordered and ordered hard-sphere packings. Phys. Rev. E. 71 (1), 011105.
Einav, I., 2007. Breakage mechanics-Part i: theory. J. Mech. Phys. Solids 55 (6), 1274–1297.
Erguler, Z.A., 2016. A quantitative method of describing grain size distribution of soils and some examples for its applications. Bull. Eng. Geol. Environ. 75 (2), 807–819.
Farr, R.S., Groot, R.D., 2009. Close packing density of polydisperse hard spheres. J. Chem. Phys. 131 (24), 244104.
Fraser, H., 1935. Experimental study of the porosity and permeability of clastic sediments. J. Geol. 43 (8, Part 1), 910–1010.
Göncü, F., Durán, O., Luding, S., 2010. Constitutive relations for the isotropic deformation of frictionless packings of polydisperse spheres. Comptes Rendus Mécanique 338 (10–11), 570–586.
Göncü, F., Luding, S., 2013. Effect of particle friction and polydispersity on the macroscopic stress–strain relations of granular materials. Acta Geotech. 8 (6), 629–643.
Guida, G., Casini, F., Viggiani, G.M.B., Andó, E., Viggiani, G., 2018. Breakage mechanisms of highly porous particles in 1d compression revealed with X-ray tomography. Géotechnique Letters. In printing.
Hardin, B.O., 1985. Crushing of soil particles. J.Geotechn.Eng. 111 (10), 1177–1192.
Jia, X., Williams, R., 2001. A packing algorithm for particles of arbitrary shapes. Powder Technol. 120 (3), 175–186.
Karatza, Z., Andò, E., Papanicolopulos, S., Ooi, J., Viggiani, G., 2017. Evolution of deformation and breakage in sand studied using X-ray tomography. Géotechnique 1, 1–11.
Kolbuszewski, J., Frederick, M., 1963. The measurement of volume change in the triaxial cell'. In: Proceedings of the European Conference on Soil Mechanics and Foundation Engineering, Wiesbaden, Germany, pp. 27–32.
Kumar, N., Imole, O.I., Magnanimo, V., Luding, S., 2014. Effects of polydispersity on the micro–macro behavior of granular assemblies under different deformation paths. Particuology 12, 64–79.
Lade, P.V., Liggio, C., Yamamuro, J.A., et al., 1998. Effects of non-plastic fines on minimum and maximum void ratios of sand. Geotech. Test. J. 21, 336–347.
Lőrincz, J., Imre, E., Gálos, M., Trang, Q., Rajkai, K., Fityus, S., Telekes, G., 2005. Grading entropy variation due to soil crushing. Int. J. Geomech. 5 (4), 311–319.
Mackenzie, J., 1950. The elastic constants of a solid containing spherical holes. Proc. Phys. Soc. London, Sect. B 63 (1), 2.
Man, W., Donev, A., Stillinger, F.H., Sullivan, M.T., Russel, W.B., Heeger, D., Inati, S., Torquato, S., Chaikin, P., 2005. Experiments on random packings of ellipsoids. Phys. Rev. Lett. 94 (19), 198001.
Marks, B., Einav, I., 2011. A cellular automaton for segregation during granular avalanches. Granul. Matt. 13 (3), 211–214.
Marks, B., Einav, I., 2015. A mixture of crushing and segregation: the complexity of grainsize in natural granular flows. Geophys. Res. Lett. 42 (2), 274–281.
Marks, B., Einav, I., 2017. A heterarchical multiscale model for granular materials with evolving grainsize distribution. Granul. Matt. 19 (3), 61.
Marks, B., Guida, G., 2018. Flow stochastic lattice model @GitHub. https://github.com/benjym/FlowSLM/. Accessed April, 2018.
McDowell, G., Bolton, M., 1998. On the micromechanics of crushable aggregates. Géotechnique 48 (5), 667–679.
Miura, K., Maeda, K., Furukawa, M., Toki, S., 1997. Physical characteristics of sands with different primary properties. Soils and Foundations 37 (3), 53–64.
Nakata, Y., Hyodo, M., Hyde, A.F., Kato, Y., Murata, H., 2001. Microscopic particle crushing of sand subjected to high pressure one-Dimensional compression.. Soil and Foundation 41 (1), 69–82.
Nakata, Y., Hyodo, M., Hyde, A.F., Kato, Y., Murata, H., 2001. One-dimensional compression behaviour of uniformly graded sand related to single particle crushing strength. Soils and Foundations 41 (2), 39–51.
Oda, M., 1972. Initial fabrics and their relations to mechanical properties of granular material. Soils and foundations 12 (1), 17–36.
Ogarko, V., Luding, S., 2013. Prediction of polydisperse hard-sphere mixture behavior using tridisperse systems. Soft Matt. 9 (40), 9530–9534.
Ogarko, V., Rivas, N., Luding, S., 2014. Communication: Structure characterization of hard sphere packings in amorphous and crystalline states.
Peronius, N., Sweeting, T., 1985. On the correlation of minimum porosity with particle size distribution. Powder Technol. 42 (2), 113–121.
Powers, M.C., 1953. A new roundness scale for sedimentary particles. J. Sediment. Res. 23 (2).
Rubin, M., Einav, I., 2011. A large deformation breakage model of granular materials including porosity and inelastic distortional deformation rate. Int. J. Eng. Sci. 49 (10), 1151–1169.
Santamarina, J., Cho, G., 2004. Soil behaviour: The role of particle shape. In: Advances in geotechnical engineering: The skempton conference, 1. Thomas Telford, London, pp. 604–617.
Senetakis, K., Anastasiadis, A., Pitilakis, K., 2012. The small-Strain shear modulus and damping ratio of quartz and volcanic sands. Geotech. Test. J. 35 (6), 1–17.
Sympatec, 2008. QICPIC. Windox-operating instruction release 5.4.1.0. Clausthal-Zellerfeld, Germany.
Tengattini, A., Das, A., Einav, I., 2016. A constitutive modelling framework predicting critical state in sand undergoing crushing and dilation. Géotechnique 66 (9), 695–710. doi:10.1680/jgeot.14.P.164.
Torquato, S., Stillinger, F.H., 2010. Jammed hard-particle packings: from kepler to bernal and beyond. Rev. Mod. Phys. 82 (3), 2633.
Torquato, S., Truskett, T.M., Debenedetti, P.G., 2000. Is random close packing of spheres well defined? Phys. Rev. Lett. 84 (10), 2064.
Viggiani, G.M.B., Atkinson, J., 1995. Stiffness of fine-grained soil at very small strains. Géotechnique 45 (2), 249–265.
Weibull, W., 1939. A statistical theory of strength of materials. IVB-Handl..
Wood, D.M., Maeda, K., 2008. Changing grading of soil: effect on critical states. Acta Geotech. 3 (1), 3.
Youd, T., 1973. Factors controlling maximum and minimum densities of sands.. ASTM STM 523 98–112.
Yu, A.B., Standish, N., 1988. An analytical-parametric theory of the random packing of particles. Powder Technol. 55 (3), 171–186.

Please cite this article as: G. Guida, I. Einav and B. Marks et al., Linking micro grainsize polydispersity to macro porosity, International Journal of Solids and Structures, https://doi.org/10.1016/j.ijsolstr.2018.11.032